Syntheses, Structures, and Magnetic Properties of Two Kinds of Unique Heterometallic Chains with Mixed-Bridging Ligands of Tricyanometalate and Alkoxide

Ling-Chen Kang, Xin Chen, Hui-Sheng Wang, Yi-Zhi Li, You Song,* Jing-Lin Zuo,* and Xiao-Zeng You

State Key Laboratory of Coordination Chemistry, School of Chemistry and Chemical Engineering, Nanjing National Laboratory of Microstructures, Nanjing University, Nanjing 210093, P. R. China

The reactions of copper(II) salts, 1,3-bis(dimethylamino)-2-propanol (bdmapH) or 1,3-bis(amino)-2-propanol (bapH) and $[(Tp)Fe(CN)_3]^-$ (Tp = tris(pyrazolyl)hydroborate) gave four mixed-bridged heterometallic one-dimensional (1D) coordination polymers, $\{[(Tp)_2Fe_2(CN)_6(OAc)(bdmap)Cu_2(H_2O)]\cdot 2H_2O\}_n$ (**1**, HOAc = acetic acid), $\{[(Tp)_2Fe_2(CN)_6(Pa)(bdmap)Cu_2(H_2O)]\cdot 2MeCN\}_n$ (**2**, HPa = propionic acid), $\{[(Tp)_2Fe_2(CN)_6(Tfa)(bdmap)Cu_2(H_2O)]\cdot 2MeCN\}_n$ (**3**, HTfa = trifluoroacetic acid), and $\{[(Tp)_2Fe_2(CN)_6(OAc)(bap)Cu_2(MeOH)]\cdot 2MeOH\cdot H_2O\}_n$ (**4**). Complexes **1**−**3** show unique branched zigzag chain structures and complex **4** exhibits as a steplike chain. Ferromagnetic interactions between Fe^{III} and Cu^{II} ions by bridging cyanides are observed in all complexes. Strong antiferromagnetic interactions are presented between the Cu^{II} ions in complexes **1**−**3**, whereas similar antiferromagnetic coupling between Cu^{II} ions is obviously weakened in complex **4** because of the distortion of penta-coordinated Cu^{II} ions.

Introduction

Cyanide, a typical linear bridging ligand,[1] is able to effectively mediate the magnetic interactions between two metal ions to some extent in the field of molecular magnetic materials, such as high-T_C magnetism,[2] photo- and electromagnetism,[3] spincrossover,[4] single-molecule magnets (SMMs),[5] and single-chain magnets (SCMs).[6] Recently, polydentate N-donor or P-donor chelating ligands have been introduced in the synthetic route for modified hexacyanometalates or octacyanometalates $[(L)M(CN)_q]^{p-}$ units, where L = polydentate organic ligands, M = V, Cr, Fe, Mo, W, Re, etc. These so-called building blocks are widely utilized to fabricate low-dimensional cyano-bridged molecular materials.[7−12] Among them, the tailored tricyanometalate precursor $[(Tp)Fe(CN)_3]^-$

---

*To whom correspondence should be addressed. E-mail: zuojl@nju.edu.cn (J.-L.Z.); yousong@nju.edu.cn (Y.S.). Fax: +86-25-83314502.

(1) (a) Dunbar, K. R.; Heintz, R. A. *Prog. Inorg. Chem.* **1997**, *45*, 283. (b) Weihe, H.; Güdel, H. U. *Comments Inorg. Chem.* **2000**, *22*, 75. (c) Miller, J. S. *MRS. Bull.* **2000**, *25*, 60. (d) Marvaud, V.; Decroix, C.; Scuiller, A.; Guyard-Duhayon, C.; Vaissermann, J.; Gonnet, F.; Verdaguer, M. *Chem.—Eur. J.* **2003**, *9*, 1677. (e) Marvaud, V.; Decroix, C.; Scuiller, A.; Tuyéras, F.; Guyard-Duhayon, C.; Vaissermann, J.; Marrot, J.; Gonnet, F.; Verdaguer, M. *Chem.—Eur. J.* **2003**, *9*, 1692. (f) Beltran, L. M. C.; Long, J. R. *Acc. Chem. Res.* **2005**, *38*, 325 and references therein. (g) Gunter, M. J.; Berry, K. J.; Murray, K. S. *J. Am. Chem. Soc.* **1984**, *106*, 4227. (h) Mazurek, W.; Kennedy, B. J.; Murray, K. S.; O'Connor, M. J.; Rodgers, J. R.; Snow, M. R.; Wedd, A. G.; Zwack, P. R. *Inorg. Chem.* **1985**, *24*, 3258. (i) Van Langenberg, K.; Batten, S. R.; Berry, K. J.; Hockless, D. C. R.; Moubaraki, B.; Murray, K. S. *Inorg. Chem.* **1997**, *36*, 5006.

(2) (a) Ferlay, S.; Mallah, T.; Quahès, R.; Veillet, P.; Verdaguer, M. *Nature* **1995**, *378*, 701. (b) Sato, O.; Iyoda, T.; Fujishima, A.; Hashimoto, K. *Science* **1996**, *271*, 49. (c) Holmes, S. M.; Girolami, G. S. *J. Am. Chem. Soc.* **1999**, *121*, 5593.

(3) (a) Sato, O.; Iyoda, T.; Fujishima, A.; Hashimoto, K. *Science* **1996**, *272*, 704. (b) Ohkoshi, S. I.; Fujishima, A.; Hashimoto, K. *J. Am. Chem. Soc.* **1998**, *120*, 5349. (c) Yokoyama, T.; Okamoto, K.; Ohta, T.; Ohkoshi, S. I.; Hashimoto, K. *Phys. Rev. B* **2002**, *65*, 064438. (d) Arimoto, Y.; Ohkoshi, S. I.; Zhong, Z. J.; Seino, H.; Mizobe, Y.; Hashimoto, K. *J. Am. Chem. Soc.* **2003**, *125*, 9240. (e) Sato, O. *Acc. Chem. Res.* **2003**, *36*, 692.

(4) (a) Niel, V.; Thompson, A. L.; Muñnoz, M. C.; Galet, A.; Goeta, A. E.; Real, J. A. *Angew. Chem., Int. Ed.* **2003**, *42*, 3760. (b) Nihei, M.; Ui, M.; Yokota, M.; Han, L.; Maeda, A.; Kishida, H.; Okamoto, H.; Oshio, H. *Angew. Chem., Int. Ed.* **2005**, *44*, 6484. (c) Shatruk, M.; Dragulescu-Andrasi, A.; Chambers, K. E.; Stoian, S. A.; Bominaar, E. L.; Achim, C.; Dunbar, K. R. *J. Am. Chem. Soc.* **2007**, *129*, 6104. (d) Li, D. F.; Clérac, R.; Roubeau, O.; Harté, E.; Mathonière, C.; Le Bris, R.; Holmes, S. M. *J. Am. Chem. Soc.* **2008**, *130*, 252.

(5) (a) Sokol, J. J.; Hee, A. G.; Long, J. R. *J. Am. Chem. Soc.* **2002**, *124*, 7656. (b) Berlinguette, C. P.; Vaughn, D.; Canada-Vilalta, C.; Galán-Mascarós, J. R.; Dunbar, K. R. *Angew. Chem., Int. Ed.* **2003**, *42*, 1523. (c) Song, Y.; Zhang, P.; Ren, X. M.; Shen, X. F.; Li, Y. Z.; You, X. Z. *J. Am. Chem. Soc.* **2005**, *127*, 3708. (d) Li, D. F.; Parkin, S.; Wang, G. B.; Yee, G. T.; Clérac, R.; Wernsdorfer, W.; Holmes, S. M. *J. Am. Chem. Soc.* **2006**, *128*, 4214. (e) Freedman, D. E.; Jenkins, D. M.; Iavarone, A. T.; Long, J. R. *J. Am. Chem. Soc.* **2008**, *130*, 2884.

(6) (a) Lescouëzec, R.; Vaissermann, J.; Ruiz-Pérez, C.; Lloret, F.; Carrasco, R.; Julve, M.; Verdaguer, M.; Dromzee, Y.; Gatteschi, D.; Wernsdorfer, W. *Angew. Chem., Int. Ed.* **2003**, *42*, 1483. (b) Toma, L. M.; Lescouëzec, R.; Lloret, F.; Julve, M.; Vaissermann, J.; Verdaguer, M. *Chem. Commun.* **2003**, 1850. (c) Toma, L. M.; Lescouëzec, R.; Pasán, J.; Ruiz-Pérez, C.; Vaissermann, J.; Cano, J.; Carrasco, R.; Wernsdorfer, W.; Lloret, F.; Julve, M. *J. Am. Chem. Soc.* **2006**, *128*, 4842. (d) Ferbinteanu, M.; Miyasaka, H.; Wernsdorfer, W.; Nakata, K.; Sugiura, K.; Yamashita, M.; Coulon, C.; Clérac, R. *J. Am. Chem. Soc.* **2005**, *127*, 3090. (e) Harris, T. D.; Bennett, M. V.; Clérac, R.; Long, J. R. *J. Am. Chem. Soc.* **2010**, *132*, 3980. (f) Lescouëzec, R.; Toma, L. M.; Vaissermann, J.; Verdaguer, M.; Delgado, F. S.; Ruiz-Pérez, C.; Lloret, F.; Julve, M. *Coord. Chem. Rev.* **2005**, *249*, 2691.

(7) Li, D. F.; Parkin, S.; Wang, G. B.; Yee, G. T.; Holmes, S. M. *Inorg. Chem.* **2006**, *45*, 2773.

(8) (a) Sokol, J. J.; Shores, M. P.; Long, J. R. *Angew. Chem., Int. Ed.* **2001**, *40*, 236. (b) Harris, T. D.; Long, J. R. *Chem. Commun.* **2007**, 1360. (c) Yang, J. Y.; Shores, M. P.; Sokol, J. J.; Long, J. R. *Inorg. Chem.* **2003**, *42*, 1403. (d) Li, D. F.; Ruschman, C.; Parkin, S.; Clérac, R.; Holmes, S. M. *Chem. Commun.* **2006**, 4036.

Scheme 1. Left, Tricyanometalate Building Block, $[(Tp)Fe(CN)_3]^-$ Unit; Right, bdmap and bap Chelated Binuclear Subunits Bridged by Alkoxy Oxygen Atom

$[(Tp)Fe(CN)_3]^-$

M = first row transition metal
R = H, Me
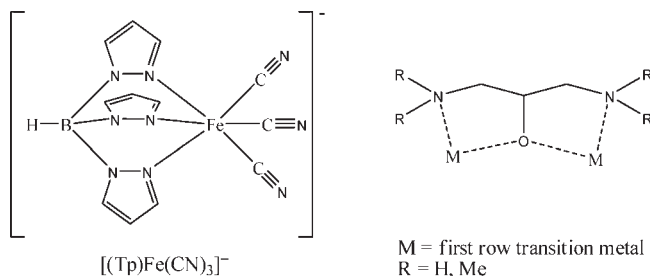
(Scheme 1) is chosen as one of the building blocks in our group for the following reasons: (i) because of the negative charge, it exhibits the virtue of good solubility and provides high-spin products with lower positive charge and improved stability; (ii) the low-spin Fe^{III} ion possesses obvious single-ion magnetic anisotropy because of the unquenched first-order orbital angular momentum,[13] which is favorable for SMMs and SCMs.[14]

Hydroxide or alkoxide are also widely used as bridging ligands to connect paramagnetic metal ions and the resulted complexes show variety of structures and rich magnetostructural correlations.[15] In some metal complexes, the bridging

oxygen atoms are even more effective in mediating magnetic interaction than cyanides.[16] Importantly, many hydroxyl- or alkoxy-bridged SMMs have also been reported.[17] Introduction of hydroxyl or alkoxy together with cyanides in the syntheses of low-dimensional magnetic complexes may possibly provide a chance for new mixed-bridged SMMs and SCMs.[18] 1,3-bis(dimethylamino)-2-propanolato (bdmap) and 1,3-bis(amino)-2-propanolato (bap) anions are able to coordinate two paramagnetic metal ions bridged by one alkoxy oxygen atom, and they are good candidates to offer stable alkoxy-bridged subunits for polymeric complexes (Scheme 1).[19] In this paper, using bdmapH or bapH and $(n\text{-}Bu_4N)[(Tp)Fe(CN)_3]$ to react with different copper(II) carboxylates, four mixed-bridged heterometallic 1D chain complexes, branched zigzag chain $\{[(Tp)_2Fe_2(CN)_6(OAc)(bdmap)Cu_2(H_2O)]\cdot 2H_2O\}_n$ (**1**, HOAc = acetic acid), $\{[(Tp)_2Fe_2(CN)_6(Pa)(bdmap)Cu_2(H_2O)]\cdot 2MeCN\}_n$ (**2**, HPa = propionic acid), and $\{[(Tp)_2Fe_2(CN)_6(Tfa)(bdmap)Cu_2(H_2O)]\cdot 2MeCN\}_n$ (**3**, HTfa = trifluoroacetic acid), and steplike chain $\{[(Tp)_2Fe_2(CN)_6(OAc)(bap)Cu_2(MeOH)]\cdot 2MeOH\cdot H_2O\}_n$ (**4**), have been synthesized. Single-crystal X-ray structural analyses reveal that they all consist of mixed-bridged linear tetranuclear clusters that are further connected by cyanides. All complexes show ferromagnetic interactions between Fe^{III} and Cu^{II} ions through bridging cyanides, whereas strong antiferromagnetic couplings are presented between the dinuclear Cu^{II} subunits in complexes **1**−**3** and weak antiferromagnetic interaction occurs in complex **4** due to the structural difference.

Experimental Section

Starting Materials. $(n\text{-}Bu_4N)[(Tp)Fe(CN)_3]$, $Cu(Pa)_2\cdot H_2O$, and $Cu(Tfa)_2\cdot 3H_2O$ were prepared according to the literature.[20,21] 1,3-Bis(dimethylamino)-2-propanol and 1,3-bis(amino)-2-propanol were purchased from Aldrich. The other materials are commercially available and were used as received.

Caution: The cyanides are very toxic. Thus, these starting materials should be handled in small quantities and with great caution.

Preparation of $\{[(Tp)_2Fe_2(CN)_6(OAc)(bdmap)Cu_2(H_2O)]\cdot 2H_2O\}_n$ (**1**). 1,3-Bis(dimethylamino)-2-propanol (7.5 mg, 0.05 mmol) was added to the solution of $Cu(OAc)_2\cdot H_2O$ (20 mg, 0.1 mmol) in 5 mL of water, leading to a dark blue solution. After stirring for 15 min, the solution of $(n\text{-}Bu_4N)[(Tp)Fe(CN)_3]$ (30 mg, 0.05 mmol) in 10 mL of MeOH was added. Dark-brown block crystals were collected by filtration after slow evaporation of the resulted solution for several days. Yield: 14 mg, 52% (based on Fe). Anal. Calcd for $C_{33}H_{46}B_2Cu_2Fe_2N_{20}O_6$ (%): C, 36.72; H, 4.30; N, 25.96. Found: C, 36.53; H, 4.41; N, 26.09.

(9) (a) Li, D. F.; Parkin, S.; Wang, G.; Yee, G. T.; Prosvirin, A. V.; Holmes, S. M. *Inorg. Chem.* **2005**, *44*, 4903. (b) Li, D. F.; Clérac, R.; Parkin, S.; Wang, G. B.; Yee, G. T.; Holmes, S. M. *Inorg. Chem.* **2006**, *45*, 5251. (c) Jiang, L.; Feng, X. L.; Lu, T. B.; Gao, S. *Inorg. Chem.* **2006**, *45*, 5018. (d) Ni, Z. H.; Kou, H. Z.; Zhang, L. F.; Ni, W. W.; Jiang, Y. B.; Cui, A. L.; Ribas, J.; Sato, O. *Inorg. Chem.* **2005**, *44*, 9631. (e) Ni, Z. H.; Kou, H. Z.; Zhao, Y. H.; Zheng, L.; Wang, R. J.; Cui, A. L.; Sato, O. *Inorg. Chem.* **2005**, *44*, 2050. (f) Ni, W. W.; Ni, Z. H.; Cui, A. L.; Liang, X.; Kou, H. Z. *Inorg. Chem.* **2007**, *46*, 22. (g) Kim, J.; Han, S.; Pokhodnya, K. I.; Migliori, J. M.; Miller, J. S. *Inorg. Chem.* **2005**, *44*, 6983. (h) Jiang, L.; Choi, H. J.; Feng, X. L.; Lu, T. B.; Long, J. R. *Inorg. Chem.* **2007**, *46*, 2181. (i) Nihei, M.; Ui, M.; Hoshino, N.; Oshio, H. *Inorg. Chem.* **2008**, *47*, 6106. (j) Zhang, Y. J.; Liu, T.; Kanegawa, S.; Sato, O. *J. Am. Chem. Soc.* **2009**, *131*, 7942. (k) Kim, J. I.; Yoo, H. S.; Koh, E. K.; Hong, C. S. *Inorg. Chem.* **2007**, *46*, 10461. (l) Kwak, H. Y.; Ryu, D. W.; Lee, J. W.; Yoon, J. H.; Kim, H. C.; Koh, E. K.; Krinsky, J.; Hong, C. S. *Inorg. Chem.* **2010**, *49*, 4632.

(10) Shores, M. P.; Sokol, J. J.; Long, J. R. *J. Am. Chem. Soc.* **2002**, *124*, 2279.

(11) (a) Yoon, J. H.; Lim, J. H.; Kim, H. C.; Hong, C. S. *Inorg. Chem.* **2006**, *45*, 9613. (b) Choi, S. W.; Kwak, H. Y.; Yoon, J. H.; Kim, H. C.; Koh, E. K.; Hong, C. S. *Inorg. Chem.* **2008**, *47*, 10214.

(12) (a) Schelter, E. J.; Bera, J. K.; Bacsa, J.; Galn-Mascars, J. R.; Dunbar, K. R. *Inorg. Chem.* **2003**, *42*, 4256. (b) Schelter, E. J.; Prosvirin, A. V.; Dunbar, K. R. *J. Am. Chem. Soc.* **2004**, *126*, 15004. (c) Schelter, E. J.; Prosvirin, A. V.; Reiff, W. M.; Dunbar, K. R. *Angew. Chem., Int. Ed.* **2004**, *43*, 4912. (d) Schelter, E. J.; Karadas, F.; Avendano, C.; Prosvirin, A. V.; Wernsdorfer, W.; Dunbar, K. R. *J. Am. Chem. Soc.* **2007**, *129*, 8139. (e) Karadas, F.; Schelter, E. J.; Shatruk, M.; Prosvirin, A. V.; Bacsa, J.; Smirnov, D.; Ozarowski, A.; Krzystek, J.; Telser, J.; Dunbar, K. R. *Inorg. Chem.* **2008**, *47*, 2074.

(13) (a) Palii, A. V.; Ostrovsky, S. M.; Klokishner, S. I.; Tsukerblat, B. S.; Dunbar, K. R. *Chem. Phys. Chem.* **2006**, *7*, 871. (b) Park, K.; Holmes, S. M. *Phys. Rev. B.* **2006**, *74*, 224440.

(14) (a) Wang, C. F.; Zuo, J. L.; Bartlett, B. M.; Song, Y.; Long, J. R.; You, X. Z. *J. Am. Chem. Soc.* **2006**, *128*, 7162. (b) Wang, S.; Zuo, J. L.; Zhou, H. C.; Choi, H. J.; Ke, Y.; Long, J. R.; You, X. Z. *Angew. Chem., Int. Ed.* **2004**, *43*, 5940. (c) Wang, S.; Zuo, J. L.; Gao, S.; Song, Y.; Zhou, H. C.; Zhang, Y. Z.; You, X. Z. *J. Am. Chem. Soc.* **2004**, *126*, 8900. (d) Wang, C. F.; Li, D. P.; Chen, X.; Li, X. M.; Li, Y. Z.; Zuo, J. L.; You, X. Z. *Chem. Commun.* **2009**, 6940.

(15) (a) Ruiz, E.; Alemany, P.; Alvarez, S.; Cano, J. *J. Am. Chem. Soc.* **1997**, *119*, 1297. (b) Ruiz, E.; Alemany, P.; Alvarez, S.; Cano, J. *Inorg. Chem.* **1997**, *36*, 3683.

(16) (a) Crawford, V. H.; Richardson, H. W.; Wasson, J. R.; Hodgson, D. J.; Hatfield, W. E. *Inorg. Chem.* **1976**, *15*, 2017. (b) Rodríguez-Fortea, A.; Alemany, P.; Alvarez, S.; Ruiz, E.; Sciuller, A.; Decroix, C.; Marvaud, V.; Vaissermann, J.; Verdaguer, M.; Rosenman, I.; Julve, M. *Inorg. Chem.* **2001**, *40*, 5868.

(17) (a) Oshio, H.; Hoshino, N.; Ito, T.; Nakano, M. *J. Am. Chem. Soc.* **2004**, *126*, 8805. (b) Oshio, H.; Nihei, M.; Yoshida, A.; Nojiri, H.; Nakano, M.; Yamaguchi, A.; Karaki, Y.; Ishimoto, H. *Chem.—Eur. J.* **2005**, *11*, 843. (c) Lecren, L.; Roubeau, O.; Coulon, C.; Li, Y. G.; Le Goff, X. F.; Wernsdorfer, W.; Miyasaka, H.; Clérac, R. *J. Am. Chem. Soc.* **2005**, *127*, 17353. (d) Yang, E. C.; Wernsdorfer, W.; Zakharov, L. N.; Karaki, Y.; Yamaguchi, A.; Isidro, R. M.; Lu, G. D.; Wilson, S. A.; Rheingold, A. L.; Ishimoto, H.; Hendrickson, D. N. *Inorg. Chem.* **2006**, *45*, 529.

(18) (a) Toma, L.; Toma, L. M.; Lescouëzec, R.; Armentano, D.; De Munno, G.; Andruh, M.; Cano, J.; Lloret, F.; Julve, M. *Dalton Trans.* **2005**, 1357. (b) Shiga, T.; Okawa, H.; Kitagawa, S.; Ohba, M. *J. Am. Chem. Soc.* **2006**, *128*, 16426.

(19) Fallah, M. S. E.; Badyine, F.; Vicente, R.; Escuer, A.; Solans, X.; Font-Bardia, M. *Dalton Trans.* **2006**, 2934.

(20) Lescouëzec, R.; Vaissermann, J.; Lloret, F.; Julve, M.; Verdaguer, M. *Inorg. Chem.* **2002**, *41*, 5943.

(21) (a) Casarin, M.; Corvaja, C.; Nicola, C. D.; Falcomer, D.; Franco, L.; Monari, M.; Pandolfo, L.; Pettinari, C.; Piccinelli, F. *Inorg. Chem.* **2005**, *44*, 6265. (b) Patel, K. S.; Faniran, J. A. *J. Inorg. Nucl. Chem.* **1976**, *38*, 1001.

Table 1. Summary of Crystallographic Data for the Complexes **1−4**

	1	**2**	**3**	**4**
formula	$C_{33}H_{46}B_2Cu_2Fe_2N_{20}O_6$	$C_{38}H_{50}B_2Cu_2Fe_2N_{22}O_4$	$C_{37}H_{45}B_2Cu_2F_3Fe_2N_{22}O_4$	$C_{32}H_{46}B_2Cu_2Fe_2N_{20}O_7$
fw	1079.30	1139.40	1179.37	1083.29
cryst syst	monoclinic	monoclinic	monoclinic	triclinic
space group	$P2_1/c$	$P2_1/c$	$P2_1/c$	$P\bar{1}$
a (Å)	20.1191(18)	20.2463(17)	20.163(2)	10.227(2)
b (Å)	10.0528(9)	10.0309(9)	10.1014(12)	13.747(3)
c (Å)	27.0261(17)	27.3713(17)	27.227(2)	18.143(4)
a (deg)	90	90	90	73.269(4)
β (deg)	116.561(5)	115.731(5)	116.002(3)	88.799(4)
γ (deg)	90	90	90	71.847(3)
V (Å^3)	4889.2(7)	5007.6(7)	4984.2(9)	2314.5(8)
Z	4	4	4	2
D_{calcd} (g cm^{-3})	1.466	1.511	1.572	1.554
T (K)	291(2)	291(2)	291(2)	291(2)
μ (mm^{-1})	1.501	1.468	1.487	1.587
θ (deg)	1.68−26.00	2.19−26.00	1.66−26.00	2.10−26.00
$F(000)$	2208	2336	2400	1108
index ranges	$-21 \leq h \leq 24$	$-24 \leq h \leq 18$	$-24 \leq h \leq 22$	$-11 \leq h \leq 12$
	$-12 \leq k \leq 11$	$-12 \leq k \leq 11$	$-12 \leq k \leq 12$	$-16 \leq k \leq 16$
	$-33 \leq l \leq 33$	$-18 \leq l \leq 33$	$-24 \leq l \leq 33$	$-22 \leq l \leq 14$
data/restraints/params	9572/0/686	9755/0/706	9734/0/655	8837/0/599
GOF (F^2)	1.051	1.082	1.136	1.055
$R_1{}^a$, $wR_2{}^b$ ($I > 2\sigma(I)$)	0.0497	0.0515	0.0538	0.0563
	0.1381	0.1151	0.0941	0.1123
$R_1{}^a$, $wR_2{}^b$ (all data)	0.0639	0.0686	0.0716	0.0760
	0.1450	0.1199	0.0982	0.1161

$^a R_1 = \Sigma ||F_o| - |F_c||/\Sigma |F_o|$. $^b wR_2 = [\Sigma w(F_o{}^2 - F_c{}^2)^2/\Sigma w(F_o{}^2)]^{1/2}$.

IR (KBr, cm^{-1}): 3428 (br), 2987 (br), 2505 (m), 2172 (s), 2140 (m), 2125 (m), 1625 (m), 1569 (vs), 1502 (s), 1467 (m), 1426 (s), 1407 (s), 1314 (s), 1214 (s), 1118 (s), 1075 (m), 1049 (vs), 989 (m), 780 (s), 711 (s), 665 (m), 617 (m).

Preparation of {[(Tp)$_2$Fe$_2$(CN)$_6$(Pa)(bdmap)Cu$_2$(H$_2$O)]·2Me-CN}$_n$ **(2).** Complex **2** as dark-brown crystals was synthesized from Cu(Pa)$_2$·H$_2$O (23 mg, 0.1 mmol), 1,3-bis(dimethylamino)-2-propanol (7.5 mg, 0.05 mmol) and (*n*-Bu$_4$N)[(Tp)Fe(CN)$_3$] (30 mg, 0.05 mmol) by following similar procedures as that described for complex **1** except that MeCN was used instead of MeOH as solvent. Yield: 12 mg, 42% (Based on Fe). Anal. Calcd for C$_{38}$H$_{50}$B$_2$Cu$_2$Fe$_2$N$_{22}$O$_4$ (%): C, 40.06; H, 4.42; N, 27.04. Found: C, 39.89; H, 4.65; N, 26.79. IR (KBr, cm^{-1}): 3426 (br), 2974 (br), 2515 (m), 2170 (m), 2139 (m), 2123 (m), 1624 (w), 1561 (vs), 1502(m), 1466(s), 1426(m), 1407 (vs), 1313 (vs), 1215 (s), 1118 (s), 1074 (m), 1048 (vs), 990 (m), 898 (m), 781 (s), 711 (s), 655 (s).

Preparation of {[(Tp)$_2$Fe$_2$(CN)$_6$(Tfa)(bdmap)Cu$_2$(H$_2$O)]·2MeCN}$_n$ **(3).** Complex **3** as dark-brown crystals was synthesized from Cu(Tfa)$_2$·3H$_2$O (34 mg, 0.1 mmol), 1,3-bis(dimethyl-amino)-2-propanol (7.5 mg, 0.05 mmol), and (*n*-Bu$_4$N)[(Tp)Fe-(CN)$_3$] (30 mg, 0.05 mmol) by following a procedure similar to that described for complex **2**. Yield: 18 mg, 61% (based on Fe). Anal. Calcd for C$_{37}$H$_{45}$B$_2$Cu$_2$F$_3$Fe$_2$N$_{22}$O$_4$ (%): C, 37.68; H, 3.85; N, 26.13. Found: C, 37.39; H, 4.05; N, 26.29. IR (KBr, cm^{-1}): 3396 (br), 3106 (br), 2509 (m), 2171 (m), 2145 (m), 2124 (m), 1665 (vs), 1502(m), 1465(s), 1431 (m), 1408 (vs), 1313 (s), 1207 (vs), 1150 (m), 1119 (m), 1075 (m), 1049 (vs), 989 (m), 921 (w), 895 (w), 782 (s), 711 (s), 652 (w).

Preparation of {[(Tp)$_2$Fe$_2$(CN)$_6$(OAc)(bap)Cu$_2$(MeOH)]·2MeOH·H$_2$O}$_n$ **(4).** Complex **4** as dark-brown crystals was synthesized from Cu(OAc)$_2$·H$_2$O (20 mg, 0.1 mmol), 1,3-bis-(amino)-2-propanol (4.7 mg, 0.05 mmol), and (*n*-Bu$_4$N)[(Tp)-Fe(CN)$_3$] (30 mg, 0.05 mmol) by following a procedure similar to that described for complex **1** except that 1,3-bis(amino)-2-propanol was used instead of 1,3-bis(dimethylamino)-2-propanol. Yield: 10 mg, 37% (based on Fe). Anal. Calcd for C$_{32}$H$_{46}$B$_2$Cu$_2$-Fe$_2$N$_{20}$O$_7$ (%): C, 35.48; H, 4.28; N, 25.86. Found: C, 35.62; H, 4.42; N, 25.99. IR (KBr, cm^{-1}): 3425 (br), 3120 (br), 2516 (m), 2166 (m), 2123 (m), 1568 (s), 1501 (m), 1426 (m), 1407 (s),

1313 (s), 1213 (s), 1117 (s),1074 (m),1050 (vs), 989 (m), 820 (s),769 (s),711 (s), 657 (w), 617 (w).

X-ray Structure Determination. The crystal structures were determined on a Siemens (Bruker) SMART CCD diffractometer using monochromated Mo *K*α radiation ($\lambda = 0.71073$ Å) at 291 K. Cell parameters were retrieved using SMART software and refined using SAINT[22] on all observed reflections. Data was collected using a narrow-frame method with scan widths of 0.30° in ω and an exposure time of 10 s/frame. The highly redundant data sets were reduced using SAINT[22] and corrected for Lorentz and polarization effects. Absorption corrections were applied using SADABS[23] supplied by Bruker. Structures were solved by direct methods using the program SHELXL-97.[24] The positions of metal atoms and their first coordination spheres were located from direct-methods *E*-maps; other non-hydrogen atoms were found in alternating difference Fourier syntheses and least-squares refinement cycles and, during the final cycles, refined anisotropically. Hydrogen atoms were placed in calculated positions and refined as riding atoms with a uniform value of U_{iso}, which are tied 1.2 or 1.5 times (for methyl group) to the parent atoms. Final crystallographic data and values of R_1 and wR_2 are listed in Table 1. Selected bond distances and angles for complexes **1−4** are listed in Tables 2 and 3 and Tables S1 and S2 in the Supporting Information, and selected hydrogen bonds are listed in Table S3 in the Supporting Information, respectively.

Physical measurements. Elemental analyses for C, H, and N were performed on a Perkin-Elmer 240C analyzer. Infrared spectra were recorded on a Vector22 Bruker Spectrophotometer with KBr pellets in the 400−4000 cm^{-1} region. Magnetic susceptibilities for all polycrystalline samples were measured with the use of a Quantum Design MPMS-XL7 SQUID magnetometer in the temperature range 1.8−300 K. Field dependences of

(22) *SAINT-Plus*, version 6.02; Bruker Analytical X-ray System: Madison, WI, 1999.
(23) Sheldrick, G. M. *SADABS: An Empirical Absorption Correction Program*; Bruker Analytical X-ray Systems: Madison, WI, 1996.
(24) Sheldrick, G. M. *SHELXTL-97*; Universität of Göttingen: Göttingen, Germany, 1997.
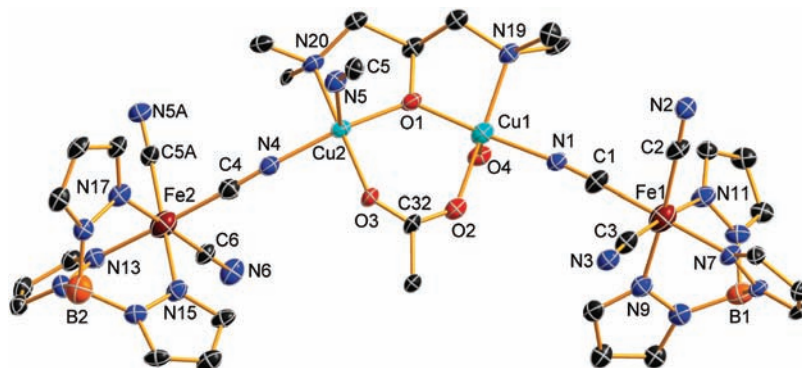
Figure 1. ORTEP view of the [(Tp)$_2$Fe$_2$(CN)$_6$(OAc)(bdmap)Cu$_2$(H$_2$O)] unit of complex **1** with an atom-numbering scheme at the 50% probability level. H atoms are omitted for clarity.

Table 2. Selected Bond Lengths (Å) and Angles (deg) for **1**[a]

Cu1—O1	1.894(2)	Cu1—N1	1.962(3)
Cu1—O2	1.976(3)	Cu1—N19	2.044(3)
Cu1—O4	2.336(3)	Cu2—O1	1.896(3)
Cu2—O3	1.957(2)	Cu2—N4	1.960(3)
Cu2—N20	2.056(3)	Cu2—N5	2.293(3)
N1—C1—Fe1	177.3(4)	N4—C4—Fe2	175.0(4)
N5—C5—Fe2#1	171.0(3)	C1—N1—Cu1	170.7(3)
C4—N4—Cu2	168.3(3)	C5—N5—Cu2	151.2(3)
O1—Cu1—N1	171.1(1)	O2—Cu1—N19	170.6(1)
O1—Cu2—N4	162.2(1)	O3—Cu2—N20	169.3(1)
Cu1—O1—Cu2	133.5(1)		

[a] Symmetry transformations used to generate equivalent atoms: #1: −x + 2, y + 1/2, −z + 3/2.

Table 3. Selected Bond Lengths (Å) and Angles (deg) for **4**[a]

Cu1—O1	1.907(3)	Cu1—O3	1.953(3)
Cu1—N1	1.995(4)	Cu1—N19	2.007(4)
Cu1—N5#1	2.270(4)	Cu2—O1	1.891(3)
Cu2—O2	1.950(3)	Cu2—N4	1.977(3)
Cu2—N20	2.004(3)	Cu2—O4	2.331(3)
N1—C1—Fe1	177.0(4)	N4—C4—Fe2	174.8(4)
N5—C5—Fe2	177.3(4)	C1—N1—Cu1	163.3(4)
C4—N4—Cu2	155.1(3)	C5—N5—Cu1#2	164.0(4)
O3—Cu1—N19	179.0(1)	O1—Cu1—N1	148.5(1)
O2—Cu2—N20	175.3(1)	O1—Cu2—N4	166.3(1)
Cu2—O1—Cu1	129.2(1)		

[a] Symmetry transformations used to generate equivalent atoms: #1: x − 1, y, z; #2: x + 1, y, z.

magnetization were measured using Quantum Design MPMS-XL5 SQUID system in an applied field up to 50 kOe.

Results and Discussions

Syntheses and IR Spectroscopic Studies. The neutral complexes **1**−**4** were synthesized through the self-assembly process by slow evaporation of the solutions containing bdmapH or bapH, (n-Bu$_4$N)[(Tp)Fe(CN)$_3$] and different copper(II) carboxylates with the molar ratio of 1:1:2. The stretching frequencies of cyanides appear at 2172, 2140, and 2125 cm^{-1} for **1**, 2170, 2139, and 2123 cm^{-1} for **2**, 2171, 2145, and 2124 cm^{-1} for **3**, 2166 and 2123 cm^{-1} for **4**, respectively, which are in good agreement with the reported bridging (2139−2172 cm^{-1}) and terminal (2123-2125 cm^{-1}) cyanides.[25] The stretching frequencies of the carboxyl are found in the range of 1560−1570 and 1426 cm^{-1} for complexes **1**, **2**, and **4**; 1665 and 1465 cm^{-1} for
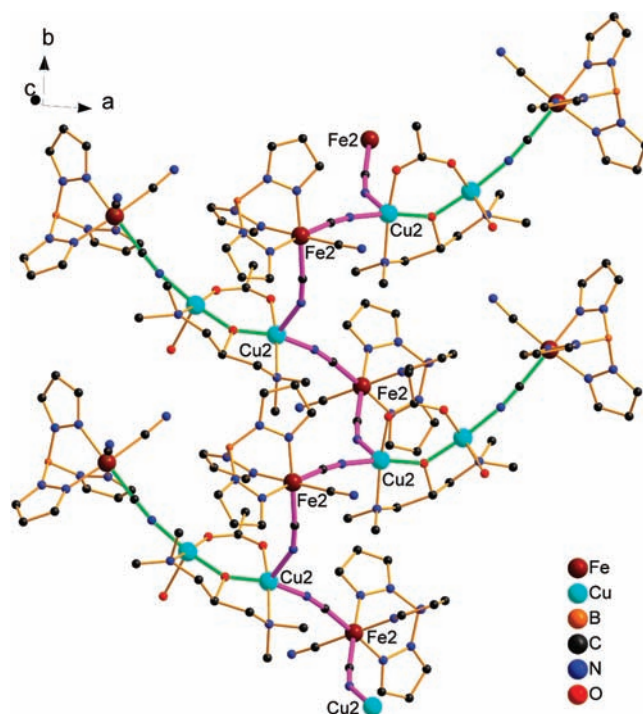

Figure 2. Perspective view of the branched zigzag chain of complex **1**. The purple lines exhibit the central cyano-bridged zigzag main chain while the light-green lines show the mixed bridged branched chains.

complex **3** related to antisymmetric ν_{as}(COO$^-$) and symmetric ν_s(COO$^-$) stretching vibrations, which fall in the normal range of the reported values.[20,26]

Structural Description. The structures of complexes **1**−**3** are quite similar. All of them are made up of neutral branched zigzag chain and solvated molecules. The main differences are the bridging carboxylic acid and solvated molecules. The ORTEP views of the asymmetry units of **1**−**3** are shown in Figure 1 and in Figures S1 and S2 in the Supporting Information, respectively. The dinuclear Cu^{II} subunit, chelated and bridged by bdmap and carboxyl, is located in the center and two [(Tp)Fe(CN)$_3$]$^-$ subunits are linked to the dinuclear Cu^{II} center by cyanides to form a linear tetranuclear Fe−Cu−Cu−Fe linkage. As shown in Figure 2 and in Figure S2 in the Supporting Information, the tetranuclear linkages are further connected to each

(25) Liu, W.; Wang, C. F.; Li, Y. Z.; Zuo, J. L.; You, X. Z. Inorg. Chem. **2006**, 45, 10058.

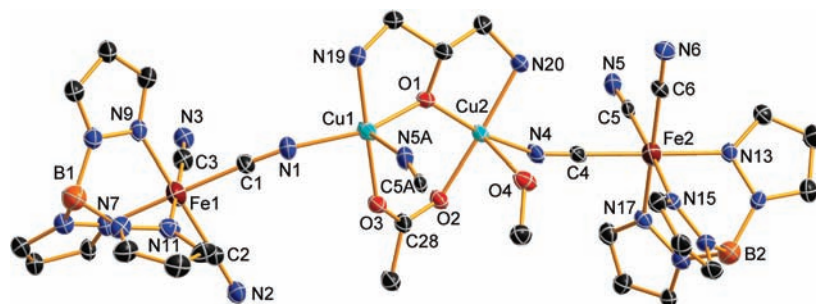(26) Breeze, S. R.; Wang, S.; Thompson, L. K. Inorg. Chim. Acta **1996**, 250, 163.

Figure 3. ORTEP view of the [(Tp)$_2$Fe$_2$(CN)$_6$(OAc)(bap)Cu$_2$(MeOH)] unit of complex **4** with an atom-numbering scheme at the 50% probability level. H atoms and solvated molecules are omitted for clarity.
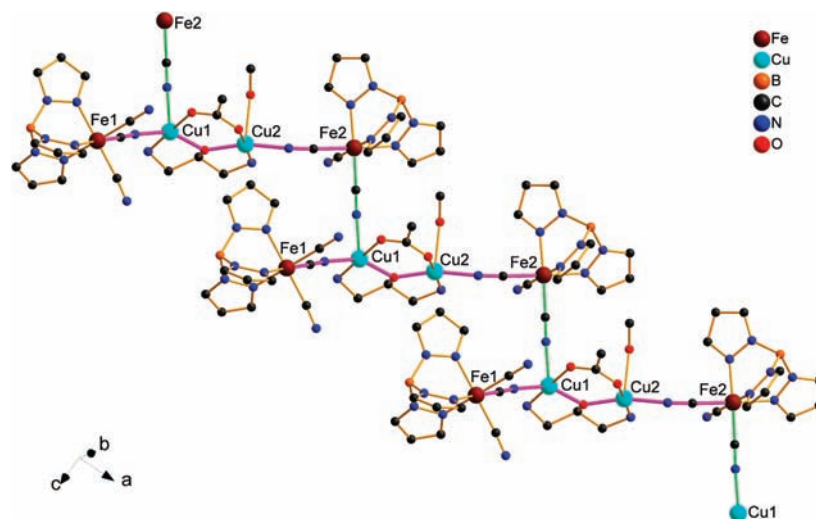

Figure 4. Perspective view of the steplike chain of complex **4**. The purple lines represent the "steps", whereas the light-green lines show the connection between the "steps".

other through Fe2−C≡N−Cu2 links to form the unique branched zigzag chain structures with the central cyano-bridged zigzag main chain (purple) and mixed-bridged branched chains (light-green). As shown in Figure S4 in the Supporting Information, racemic chains can be found in complexes **1**−**3** with crystallographic inversion centers. The Fe^{III} ions show distorted octahedral coordination environment as previously described.[20] The Cu1 atom is in penta-coordinated N$_2$O$_3$ environment forming regular square pyramidal geometry, and the trigonality indexes[27] (τ) are 0.01, 0.05, and 0.03 for complexes **1**−**3**, respectively. The Cu2 atom is penta-coordinated with N$_3$O$_2$ environment, showing slightly distorted square pyramidal geometry with τ = 0.12, 0.16, 0.16 for **1**−**3**, respectively. In the basal positions of Cu ions, the Cu1−N1 and Cu2−N4 (N1 and N4 from cyanides) distances are around 1.96 Å, whereas the bond length of Cu−N5 (from cyanide) in the apical position of Cu2 is obviously longer (about 2.25 Å). The cyanide bridges deviate from linearity differently mainly due to the benter Cu−N≡C bonds (150−170°). The Cu1−O1−Cu2 angle of the alkoxy bridge is around 133°. All the bond lengths and bond angles are within the normal values and in good agreement with other related complexes.[19,25,26]

As shown in Figure S5 in the Supporting Information, the branched chains are further connected by intrachain

hydrogen bonds to form the chains of double-rings along the *b* axis. The shortest intrachain Fe···Cu, Cu···Cu, and Fe···Fe distances are around 5.0, 3.5, and 8.6 Å, whereas the shortest interchain Fe···Cu, Cu···Cu, and Fe···Fe separations are about 7.5, 10.3, and 7.9 Å, respectively.

Complex **4** also consists of neutral chains and solvated molecules. As shown in Figure 3, the asymmetry unit of **4** is also made of linear tetranuclear units as complexes **1**−**3**. However, as shown in Figure 4, the linear tetranuclear linkages are further connected through Fe2−C≡N−Cu1 links to form a steplike chain structure. The purple lines represent the "steps" while the light-green lines show the connection between the "steps". On the other hand, as shown in Figure S6 in the Supporting Information, the structure of **4** can also be regarded as the branched zigzag chain with mixed-bridged main chain and cyano-bridged branched chains. The Fe^{III} ions possess distorted octahedral coordination geometry as that of the reported complex.[20] The Cu1 atom is penta-coordinated with τ=0.51, indicating the obvious distortion from the regular square pyramidal to trigonal bipyramidal geometry, and the Cu2 atom is penta-coordinated with the distorted square pyramidal geometry (τ = 0.15). The Cu−N$_{cyano}$ bond lengths are in the range of 1.977(3)−2.270(4) Å. The Cu−C≡N bond angles (155.1(3)−164.0(4)°) are significantly deviated from linearity, and the Cu1−O1−Cu2 angle of the alkoxy bridge is 129.2(1)°. The values of the bond lengths and bond angles fall in the normal range.[19,25]

(27) Addison, A. W.; Rao, T. N.; Reedijk, J.; van Rijn, J.; Verschoor, G. C. *Dalton Trans.* **1984**, 1349.
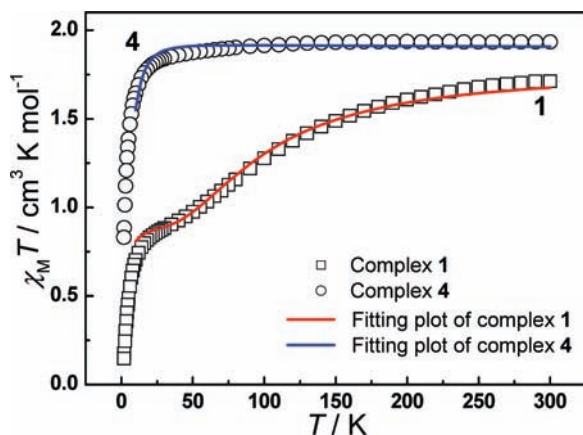
Figure 5. Temperature dependence of the $\chi_M T$ product for **1** and **4** at 2 kOe. Solid lines represent the fitting results with the uniform chain model between 10 and 300 K.

As shown in Figure S7 in the Supporting Information, a network was constructed by interchain hydrogen-bonding interactions. The shortest intrachain Fe···Cu, Cu···Cu, and Fe···Fe distances are 4.893(1), 3.432(1), and 8.234(2) Å, respectively, whereas the shortest interchain Fe···Cu, Cu···Cu, and Fe···Fe separations are 6.124(1), 8.724(2), and 6.971(1) Å, respectively.

Magnetic Properties. Magnetic measurements were performed on polycrystalline samples of complexes **1**–**4** in 1.8–300 K.

Complexes **1**–**3** exhibit similar magnetic behavior as shown in Figure 5, Figures S8–S10 in the Supporting Information. At 300 K, the $\chi_M T$ values are 1.71 cm³ K mol⁻¹ for **1** and **3**, and 1.76 cm³ K mol⁻¹ for **2**, respectively, which is higher than the spin-only value of 1.50 cm³ K mol⁻¹ ($g = 2.0$) expected for two low-spin Fe^{III} ($S = 1/2$) and two Cu^{II} ($S = 1/2$) ions in the absence of any exchange coupling, mainly ascribed to the spin−orbital coupling of low-spin octahedral Fe^{III} ions.[28] As the temperature decrease, $\chi_M T$ values quickly decrease and reach 0.92 cm³ K mol⁻¹ for **1**, 0.93 cm³ K mol⁻¹ for **2** and **3** at 40 K, respectively, suggesting the presence of significant antiferromagnetic interaction. The decreasing of $\chi_M T$ values becomes slowly in the temperature range of 15−40 K and then, below 15 K, they sharply decrease to 0.15 cm³ K mol⁻¹ for **1**, 0.10 cm³ K mol⁻¹ for **2**, and 0.13 cm³ K mol⁻¹ for **3** at 1.8 K, respectively, which may result from intermolecular antiferromagnetic interactions. And the maxima within 3.5−4.5 K in χ_M vs T plots for complexes **1**–**3** were observed, which indicate the presence of net antiferromagnetic couplings. Field dependence of magnetization of complex **1** between 0 and 50 KOe was shown in Figure 6. The M value reaches 1.18 $N\beta$ mol⁻¹ at 50 KOe and is far below the noninteracting $S = 2S_{Fe}^{III} + 2S_{Cu}^{II}$ state, which confirms the existence of antiferromagnetic interactions.

For complexes **1**–**3**, in order to describe the magnetic susceptibilities of these uniform chain systems, four J parameters within the chain, in theory, are needed (Scheme 2, left), which may easily lead to overparameterization. However, due to the C_3 symmetry of the [(Tp)Fe(CN)₃]⁻ units, all the Fe−C bond lengths and

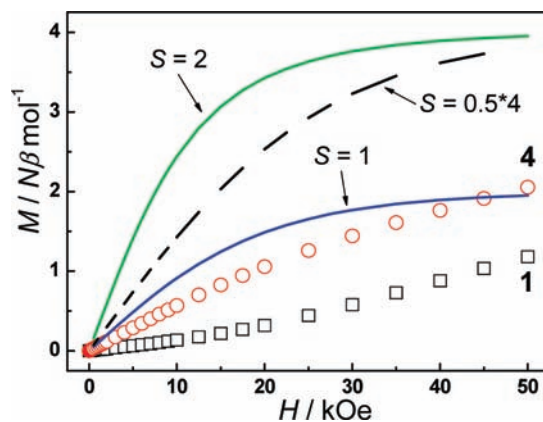(28) Carlin, R. L. *Magnetochemistry*; Springer-Verlag: New York, 1986.

Figure 6. Field dependence of magnetization of **1** (black squares) and **4** (red circles) at 1.8 K. The lines represents the Brillouin functions that corresponds to $S = 1$ (blue solid), $S = 2$ (green solid) states and noninteracting $S = 2S_{Fe}^{III} + 2S_{Cu}^{II}$ (black break) and with $g = 2.0$.

Fe−C≡N bond angles are approximately identical. Thus, J_1 and J_3 may be approximately equal because of the comparable Cu−N bond lengths (around 1.95 Å) and Cu−N≡C bond angles (around 170°) in **1**−**3**. The approximate model of the tetramer units is shown in Scheme 2 (bottom). Simultaneously, J_4 may be expected to be much smaller than J_1 and J_3, because N5 coordinates to the axial position of Cu2 atom (square pyramidal) with a longer Cu2−N5 distance (around 2.25 Å) as well as the benter Cu2−N5≡C5 bond (about 150°).[29]

The isotropic spin Hamiltonian of the tetramer is $\hat{H} = -2J_1(\hat{S}_{Fe1}\hat{S}_{Cu1} + \hat{S}_{Fe2}\hat{S}_{Cu2}) - 2J_2\hat{S}_{Cu1}\hat{S}_{Cu2}$, which can be solved following the literature[30] to give Eq 1

$$\chi_{tetra} = \frac{Ng^2\beta^2}{3kT}\frac{A}{B} \qquad (\text{Eq 1})$$

Where $A = 30\exp(-E_1/kT) + 6\exp(-E_2/kT) + 6\exp(-E_3/kT) + 6\exp(-E_4/kT)$, $B = 5\exp(-E_1/kT) + 3\exp(-E_2/kT) + 3\exp(-E_3/kT) + 3\exp(-E_4/kT) + \exp(-E_5/kT) + \exp(-E_6/kT)$,

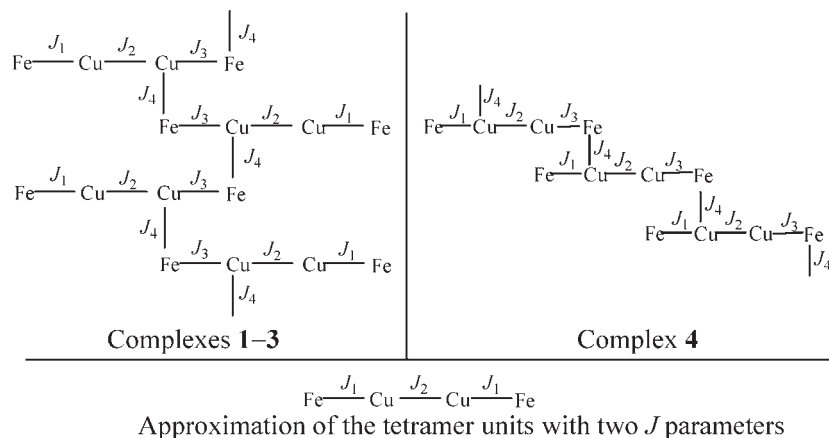$$E_1 = -J_1 - \frac{1}{2}J_2, E_2 = J_1 - \frac{1}{2}J_2$$

$$E_3 = \frac{1}{2}J_2 + \sqrt{J_1^2 + J_2^2}, E_4 = \frac{1}{2}J_2 - \sqrt{J_1^2 + J_2^2}$$

$$E_5 = \left(J_1 + \frac{1}{2}J_2\right) + \sqrt{4J_1^2 + J_2^2 - 2J_1J_2},$$

$$E_6 = \left(J_1 + \frac{1}{2}J_2\right) - \sqrt{4J_1^2 + J_2^2 - 2J_1J_2}$$

(29) (a) Toma, L.; Lescouëzec, R.; Vaissermann, J.; Delgado, F. S.; Ruiz-Pérez, C.; Carrasco, R.; Cano, J.; Lloret, F.; Julve, M. *Chem.—Eur. J.* **2004**, *10*, 6130. (b) Toma, L.; Toma, L. M.; Lescouëzec, R.; Armentano, D.; De Munno, G.; Andruh, M.; Cano, J.; Lloret, F.; Julve, M. *Dalton Trans.* **2005**, 1357.

(30) (a) Escuer, A.; Kumar, S. B.; Font-Bardia, M.; Solans, X.; Vicent, R. *Inorg. Chim. Acta* **1999**, *286*, 62. (b) Rubenacker, G. V.; Drumheller, J. E.; Emerson, K.; Willet, R. D. *J. Magn. Magn. Mater.* **1986**, *54*, 1483.

Scheme 2. Schematic Diagrams Representing the Exchange Interactions within Complexes **1−4** (top) and Approximation of the Tetramer Unit with Two *J* Parameters

Complexes 1–3 | Complex 4

$$\text{Fe} \xrightarrow{J_1} \text{Cu} \xrightarrow{J_2} \text{Cu} \xrightarrow{J_1} \text{Fe}$$

Approximation of the tetramer units with two *J* parameters

J_4 represents the magnetic interactions between the tetramers with the uniform chain model (Eq 2)[31]

$$\chi_{chain} = \frac{Ng^2\beta^2}{3kT} \frac{1+u}{1-u} S_{tetra}(S_{tetra}+1) \qquad (Eq\ 2)$$

Where $u = \coth(J_4 S_{tetra}(S_{tetra}+1)/kT) - kT/J_4 S_{tetra}(S_{tetra}+1)$, $S_{tetra}(S_{tetra}+1) = \frac{A}{B}$.

The $\chi_M T$ *vs* T plots between 10 and 300 K are fitted by the above expressions with a mean-field correction (zj') and the best fitting results are $g = 2.22$, $J_1 = J_3 = 12.6$ cm^{-1}, $J_2 = -71.1$ cm^{-1}, $J_4 = 0.21$ cm^{-1} and $zj' = -0.73$ cm^{-1} ($R = \Sigma[\chi_M T)_{calcd} - (\chi_M T)_{obsd}]^2/\Sigma(\chi_M T)_{obsd}^2 = 1.2 \times 10^{-3}$) for complex **1**; $g = 2.24$, $J_1 = J_3 = 14.4$ cm^{-1}, $J_2 = -72.4$ cm^{-1}, $J_4 = 0.22$ cm^{-1}, and $zj' = -0.65$ cm^{-1} ($R = 1.8 \times 10^{-3}$) for complex **2**; $g = 2.25$, $J_1 = J_3 = 13.7$ cm^{-1}, $J_2 = -92.1$ cm^{-1}, $J_4 = 0.22$ cm^{-1}, and $zj' = -0.77$ cm^{-1} ($R = 1.3 \times 10^{-3}$) for complex **3**, respectively.

The accuracy of the above fitting results is not satisfactory enough since J_4 is even smaller than the mean-field correction zj'. A further cutting down of the parameters may be helpful to improve the accuracy of the fitting results. Thus, the $\chi_M T$ vs T plots between 40−300 K for complexes **1−3** are also fitted with the approximate tetranuclear model in Scheme 2 (bottom) to eliminate J_4 and zj'. And the fitting results (see Figures S11−S13 in the Supporting Information) with improved R factors are $g = 2.24$, $J_1 = J_3 = 10.4$ cm^{-1}, $J_2 = -79.8$ cm^{-1} ($R = 6 \times 10^{-5}$) for **1**; $g = 2.28$, $J_1 = J_3 = 11.3$ cm^{-1}, $J_2 = -83.1$ cm^{-1} ($R = 2.4 \times 10^{-4}$) for **2**; and $g = 2.28$, $J_1 = J_3 = 12.8$ cm^{-1}, $J_2 = -105.9$ cm^{-1} ($R = 2.7 \times 10^{-4}$) for **3**, respectively.

Though the J_4 values are in doubt, the J_1 and J_3 values in both models, falling in the range of 10−15 cm^{-1}, are close to the values in reported complexes with good linearity of the cyanide linkages.[25,32] The J_2 values (−70 to −110 cm^{-1}) are also in good agreement with those reported alkoxide and carboxylate bridged copper(II) complexes,[33] confirming the strong antiferromagnetic coupling between two square pyramidal Cu^{II} centers.

The $\chi_M T$ vs T plot of complex **4** is also shown in Figure 5. At 300 K, the $\chi_M T$ value is 1.93 cm^3 K mol^{-1}, which is higher than the spin-only value of 1.50 cm^3 K mol^{-1} ($g = 2.0$) expected for two low-spin Fe^{III} ($S = 1/2$) and two Cu^{II} ($S = 1/2$) ions without any interactions, also due to the spin−orbital coupling of the low-spin octahedral Fe^{III} ions.[28] Different from complexes **1−3**, as the temperature decrease, the $\chi_M T$ value nearly keeps constant to 100 K and decreases slowly to 1.80 cm^3 K mol^{-1} at 20 K. Then, it decreases sharply to 0.83 cm^3 K mol^{-1} at 1.8 K, indicating the presence of antiferromagnetic interactions. In the M vs H plot (Figure 6), the M value reaches 2.05 Nβ mol^{-1} at 50 KOe and is far below the noninteracting $S = 2S_{Fe}^{III} + 2S_{Cu}^{II}$ state, which confirms the existence of antiferromagnetic interactions.

For complex **4**, four *J* parameters are still needed (Scheme 2, right) to describe the magnetic coupling interactions of the step-like chain. Through analysis of the magnetic properties related to bond lengths and bond angles, no similar approximation as that for complexes **1−3** can be made. Thus, to avoid overparameterization, we simply assume J_1, J_3, and J_4 are equal and the above-mentioned uniform chain model for complexes **1−3** is also applied here. The $\chi_M T$ vs T plots between 10 and 300 K is fitted to give $g = 2.26$, $J_1 = J_3 = J_4 = 1.4$ cm^{-1}, $J_2 = -7.4$ cm^{-1} and $zj' = -0.77$ cm^{-1} ($R = 1.1 \times 10^{-3}$). Simultaneously, owing to the long apical Cu1−N5 distance, the $\chi_M T$ vs T plots between 40−300 K is also fitted with the approximate tetranuclear model to neglect J_4, giving $g = 2.28$, $J_1 = J_3 = 2.7$ cm^{-1}, $J_2 = -8.5$ cm^{-1} with $R = 2 \times 10^{-5}$, as shown in Figure S14 in the Supporting Information.

As shown in Figure 5, for complex **4**, the $\chi_M T$ value nearly keeps in constant from 300 to 100 K, indicating the absence of strong antiferromagnetic coupling comparing to those of complexes **1−3**. From 100 to 20 K, the $\chi_M T$ value decreases slightly, which may be attributed to the overall effects of the antiferromagnetic interaction between the alkoxide and carboxylate bridged Cu^{II} ions and the ferromagnetic interactions between cyano bridged Fe^{III} and Cu^{II} ions. The trend of decreasing of $\chi_M T$ value, caused by antiferromagnetic interactions, is neutralized by the total ferromagnetic interactions which give ascending trend of $\chi_M T$ value and the absolutely values of J_1, J_2, J_3, and J_4 may be comparable and perhaps in the same

(31) (a) Cortés, R.; Drillon, M.; Solans, X.; Lezama, L.; Rojo, T. *Inorg. Chem.* **1997**, *36*, 677. (b) Drillon, M.; Coronado, E.; Beltrán, D.; Georges, R. *Chem. Phys.* **1983**, *79*, 449.

(32) Wang, S.; Zuo, J. L.; Zhou, H. C.; Song, Y.; Gao, S.; You, X. Z. *Eur. J. Inorg. Chem.* **2004**, 3681.

(33) Nishida, Y.; Kida, S. *Dalton Trans.* **1986**, 2633.

magnitude. Though it is difficult to get the individual values of J_1, J_3, and J_4 with enough accuracy, the plausible and averaged values of J_1, J_3, and J_4 (uniform chain) or J_1 and J_3 (tetranuclear) are close to that of previously reported complexes with bent Fe$-$C$\equiv$N$-$Cu linkage.[34] The $|J_2|$ value (<10 cm^{-1}) in complex **4** is much smaller than that in complexes **1**$-$**3**, possibly resulting from the distortion of Cu1 ion.

For complexes **1**$-$**3**, the SOMOs of Cu1 and Cu2 are $d_{x^2-y^2}$ based on slightly distorted square pyramidal geometry. Good pathway of superexchange interaction is generated, and it transmits strong antiferromagnetic coupling between the Cu ions. For complex **4**, Cu2 ($\tau = 0.15$) still exhibits slightly distorted square pyramidal geometry with $d_{x^2-y^2}$ as SOMO, whereas Cu1 ($\tau = 0.51$) is significantly distorted from regular square pyramidal geometry to trigonal bipyramid. The single e_g electron of Cu1 partially populates in d_{z^2} orbital, which is unfavorable for antiferromagnetic interaction with the $d_{x^2-y^2}$ orbital of Cu2 ion. Thus, in complex **4**, the antiferromagnetic interaction between the Cu ions is obviously reduced. In the literature, for the same reason, even ferromagnetic coupling between the alkoxide and carboxylate bridged Cu ions is observed.[35]

---

(34) Li, X. M.; Wang, C. F.; Ji, Y.; Kang, L. C.; Zhou, X. H.; Zuo, J. L.; You, X. Z. *Inorg. Chem.* **2009**, *48*, 9166.

(35) Fernandes, C.; Neves, A.; Bortoluzzi, A. J.; Mangrich, A. S.; Rentschler, E.; Szpoganicz, B.; Schwingel, E. *Inorg. Chim. Acta* **2001**, *320*, 12.

Conclusion

In summary, four new mixed-bridged heterometallic chain complexes are obtained in similar reactions and they are characterized by X-ray structure analyses and magnetic measurements. Ferromagnetic interactions are found between Fe^{III} and Cu^{II} ions through cyanides linkage in all complexes. Strong antiferromagnetic interactions, as expected, are observed between the Cu^{II} ions in complexes **1**$-$**3**. However, in complex **4**, the antiferromagnetic coupling between the Cu^{II} ions is much weakened because of the distortion of penta-coordinated Cu ions. These complexes represent new examples of heterometallic chains with mixed bridging cyano and alkoxy ligands, and the synthetic routine provide a possible way for the further preparation of new mixed bridged SCMs.

Supporting Information Available: Additional structure and magnetic characterization data (PDF), and X-ray crystallographic files in CIF format for **1**$-$**4** (PDF). This material is available free of charge via the Internet at http://pubs.acs.org.